Article Title: Adapting C_4 photosynthesis to atmospheric change and increasing productivity by elevating Rubisco content in Sorghum and Sugarcane.

Authors and Affiliations:

Coralie E. Salesse-Smith[1,3], Noga Adar[1], Baskaran Kannan[4,5], Thaibinhduong Nguyen[4,5], Wei Wei[1], Ming Guo[6,7], Zhengxiang Ge[6,7], Fredy Altpeter[4,5], Tom E. Clemente[6,7], and Stephen P. Long[1,2,3]

[1]Carl R. Woese Institute for Genomic Biology, University of Illinois at Urbana-Champaign, Urbana, IL, USA; [2]Departments of Plant Biology and of Crop Sciences, University of Illinois at Urbana-Champaign, Urbana, IL, USA; [3]DOE Center for Advanced Bioenergy and Bioproducts Innovation, Urbana-Champaign, IL, USA; [4]Agronomy Department, Plant Molecular and Cellular Biology Program, Genetics Institute, University of Florida, IFAS, Gainesville, Florida, USA; [5]DOE Center for Advanced Bioenergy and Bioproducts Innovation, Gainesville, FL, USA; [6]Department of Agronomy and Horticulture, University of Nebraska-Lincoln, Lincoln, NE, USA; [7]DOE Center for Advanced Bioenergy and Bioproducts Innovation, Lincoln, NE, USA

Corresponding authors:

Coralie E. Salesse-Smith, ces343@illinois.edu

Stephen P. Long, slong@illinois.edu

Classification:

Biological Sciences, Plant Biology

Keywords: Atmospheric change; Future-proofing agriculture; Rising CO_2; Rubisco, C_4 photosynthesis, Bundle sheath leakiness; Photosynthetic induction; CO_2 assimilation, RAF1, Transgenic field trial, Sorghum, Sugarcane

Abstract

Meta-analyses and theory show that with rising atmospheric [CO_2], Rubisco has become the greatest limitation to light-saturated leaf CO_2 assimilation rates (A_{sat}) in C_4 crops. So would transgenically increasing Rubisco increase A_{sat} and result in increased productivity in the field? Here, we successfully overexpressed the Rubisco small subunit (*RbcS*) with Rubisco accumulation factor 1 (*Raf1*) in both sorghum and sugarcane, resulting in significant increases in Rubisco content of 13-25% and up to 90% respectively. A_{sat} increased 12-15% and Rubisco enzyme activity ~40% in three independent transgenic events of both species. Sorghum plants also showed increased speeds of photosynthetic induction and decreased bundle sheath leakiness. These improvements translated into average increases of 15.5% in biomass in field-grown sorghum and a 37-81% increase in greenhouse-grown sugarcane. This suggests a potential opportunity to achieve substantial increases in productivity of this key economically important clade of C_4 crops, future proofing their value under global atmospheric change.

Significance Statement

The world is projected to need a 60% increase in food supply by 2050 (UN), and this must be achieved under conditions of global change without expanding onto yet more land. C_4 crops, while few in number, account for a large proportion of agricultural productivity. We reason that rising atmospheric [CO_2] has very recently made Rubisco, the enzyme used for all carbon fixation in plants, the greatest limitation to light saturated photosynthesis in C_4 crops. We demonstrate that transgenically increasing Rubisco content in sorghum and sugarcane, increases their photosynthetic efficiency and productivity, including in a field trial of sorghum. This shows a means to sustainably increase the productivity of this key group of crops.

68 **Introduction**

69 While very few of the 161 crop species listed by UN-FAO use C_4 photosynthesis, their
70 importance and potential in terms of global food, feed and biomass production is exceptional
71 (1). For total global biomass harvested, sugarcane (*Saccharum* hybrids) is number one and
72 maize (*Zea mays* L.) number one for seed harvested (1, 2). Sorghum (*Sorghum bicolor*) is the
73 fourth most important cereal in global production, only behind, maize, rice and wheat, but it is
74 the major cereal of the semi-arid tropics (1). While grown for biomass, the C_4 crops energycane
75 and Miscanthus show exceptional productivity (3-6). These crops all belong to the
76 monophyletic grass tribe Andropogonae.

77 The leaves of C_4 plants contain an outer layer of mesophyll cells surrounding the bundle sheath
78 cells. CO_2 diffuses from the sub-stomatal cavity into the mesophyll cytoplasm, where it
79 combines with phosphoenolpyruvate (PEP) to form oxaloacetate (OAA), catalyzed by
80 cytoplasmic PEP carboxylase (PEPC). OAA is reduced to malate in the mesophyll chloroplasts
81 and then diffuses to the bundle sheath where it is decarboxylated by $NADP^+$-dependent malic
82 enzyme (NADP-ME) creating a high [CO_2] around Ribulose-1:5 bisphosphate
83 carboxylase/oxygenase (Rubisco). The decarboxylation product, pyruvate, diffuses back to the
84 mesophyll where, catalyzed by Pyruvate Pi dikinase (PPDK), it is phosphorylated to PEP at the
85 expense of 2 ATP, completing the photosynthetic C_4 cycle (7). This photosynthetic C_4 cycle is in
86 effect a light energy driven CO_2 pump that elevates the [CO_2] around Rubisco to a level that is
87 sufficient to competitively inhibit oxygenation, preventing photorespiration and avoiding the
88 significant losses of photosynthetic efficiency that this causes in C_3 species (8). Its benefits are
89 such that considerable effort is being placed into engineering the C_4 pathway into C_3 crops (9-
90 11). Tests under open-air conditions using Free-Air Concentration Enrichment (FACE)
91 technology, have shown that higher [CO_2] increases the photosynthetic efficiency, and in turn
92 productivity, of C_3 crops, but not these C_4 crops (12-16). Thus, rising atmospheric [CO_2] could
93 progressively erode the current production advantage of C_4 plants (17). However, analysis of
94 metabolic and physiological limitations indicate that C_4 plants could be modified to also gain
95 photosynthetic efficiency at today's and future atmospheric [CO_2] (18-20).

96 Light-saturated leaf CO_2 assimilation rates (A_{sat}) in C_4 plants rise sharply with intercellular CO_2
97 concentration (C_i) to a plateau, where A_{sat} remains constant with further increase in C_i (7). In
98 maize crops grown in the field at both ambient and elevated atmospheric CO_2, this transition
99 was shown to occur at a C_i of about 120 µmol mol^{-1}, above which A_{sat} is [CO_2]-saturated (15). A
100 meta-analysis of 842 measured A-C_i responses in 49 C_4 species showed the point of CO_2
101 saturation is consistent across a broad range of C_4 species, and unaffected by growth at either
102 sub-ambient or supra-ambient [CO_2] (19). Because of their lower stomatal conductance (g_s)
103 relative to A_{sat}, the drawdown of [CO_2] between the atmosphere (C_a) and intercellular air space
104 (C_i) is greater in C_4 leaves, resulting in a ratio (C_i/C_a) of about 0.4, compared to 0.7 in C_3 species.

105 These ratios in non-water stressed plants are apparently unaffected by the [CO_2] of the growth
106 environment (12). At today's C_a of 428 µmol mol^{-1} (21), C_i in photosynthesizing C_4 leaves should
107 be about 170 µmol mol^{-1}. Therefore, at current and future atmospheric [CO_2], C_4
108 photosynthesis is [CO_2] saturated. Historically this was not the case. The average C_a of the last
109 40,000 years in which our crop ancestors evolved was 220 µmol mol^{-1} and assuming a C_i/C_a, of
110 0.4 under these conditions average C_i would have been 88 µmol mol^{-1}, well below the indicated
111 saturation point of about 120 µmol mol^{-1} (12, 22). At this C_i photosynthesis would be operating
112 on the initial slope of the response of A to C_i. The mechanistic steady-state mathematical model
113 of C_4 photosynthesis shows that this initial slope is determined by the activity of PEPC and
114 mesophyll conductance (g_m); g_m being the ease with which CO_2 can diffuse from the sub-
115 stomatal cavity into the mesophyll cytoplasm (7). The plateau however, is limited by the activity
116 of Rubisco, and potentially electron transport (7). Recent non-steady state metabolic modeling
117 and measurements show Rubisco activity also having significant control over the efficiency of
118 photosynthesis in fluctuating light (23, 24). Consistent with these predictions, transgenic knock-
119 down studies showed metabolic control of the initial slope of the A-C_i response to reside with
120 PEPC activity and the plateau shared by Rubisco and PPDK, with Rubisco accounting for 70% of
121 the control (25). This indicates that upregulation of Rubsico would increase A_{sat} in today's
122 elevated [CO_2] atmosphere.

123 Form I Rubisco, found in plants, is made up from eight small subunits (SS) encoded by the
124 nuclear gene family *RbcS* and eight large subunits (LS) encoded by the chloroplast gene *rbcL*.
125 Previously, transgenic increase in Rubisco content, by overexpression of the Rubisco small-
126 subunit (*RbcS*) and Rubisco accumulation factor 1 (*Raf1*) genes, increased A_{sat} and plant growth
127 of maize under optimal and chilling growth conditions (26, 27). However, this was confined to a
128 single hybrid genotype of maize grown in controlled environments. To test the hypothesis that
129 this improvement would be more generally possible across this key economic clade of crops
130 and result in increased productivity in the field and greenhouse, Rubisco was upregulated in
131 both sorghum and sugarcane.

132

133 **Results**

134 **Transgenic upregulation of *RbcS* and *Raf1* genes increases Rubisco abundance in sorghum and**
135 **sugarcane**

136 Two transgenes, each designed to upregulate *RbcS* and *Raf1*, were stably transformed into
137 sorghum and sugarcane (Fig.1a). The construct transformed into sorghum contains constitutive
138 promoters, while the one transformed into sugarcane contains bundle sheath specific
139 promoters as well as C-terminal epitope tags FLAG and HA. For sorghum, 9 transgenic events
140 were received and 7 determined to be single insertion lines. Transgene expression was
141 confirmed by copy number analysis and Western blot (Figure S1a). T1 plants from 7 events

142 were screened for increased CO_2 assimilation (*A*) and Rubisco activity ($V_{c,max}$) using gas
143 exchange (Fig. S1b-g). For sugarcane, 49 transgenic events were received and analyzed via
144 Western blot and a subset of events screened for improved *A* and $V_{c,max}$ (Fig. S2). The top three
145 performing events from each species based on gas exchange and protein data were then
146 characterized along with a wild-type (WT), from which the transformants were derived,
147 propagated alongside these. In sorghum, homozygous plants were obtained from each single
148 insertion event (hn1a, zg12a and zg5b) at T2. Commercial sugarcane is clonally propagated,
149 and the three events (3, 9, and 25) were effectively clones of the T0 events.

150 qPCR confirmed transgene expression in sorghum lines characterized in both the greenhouse
151 and field. All three transgenic events showed high levels of *ZmRbcS* and *ZmRaf1* expression,
152 with none in the WT (Fig. S3a-d). Immunoblots similarly showed high RAF1 protein expression
153 in the transgenic lines relative to WT (Fig. 1b). Epitope tags showed expression of sorghum SS
154 and RAF1 proteins in the sugarcane transformants (Fig. 1c).

155 Rubisco content, measured by the ^{14}C-CABP binding assay, was significantly increased by 13-
156 25% in sorghum, and by 90% and 39% in sugarcane events 3 and 25 respectively (Fig. 1d,e). No
157 significant increase was measured in event 9, even though immunoblots showed the presence
158 of the recombinant SS and RAF1, although the latter at lower levels than in events 3 and 25 (Fig.
159 1c). There were no differences in total soluble protein between WT and transgenic plants in
160 either sorghum or sugarcane (Table S3).

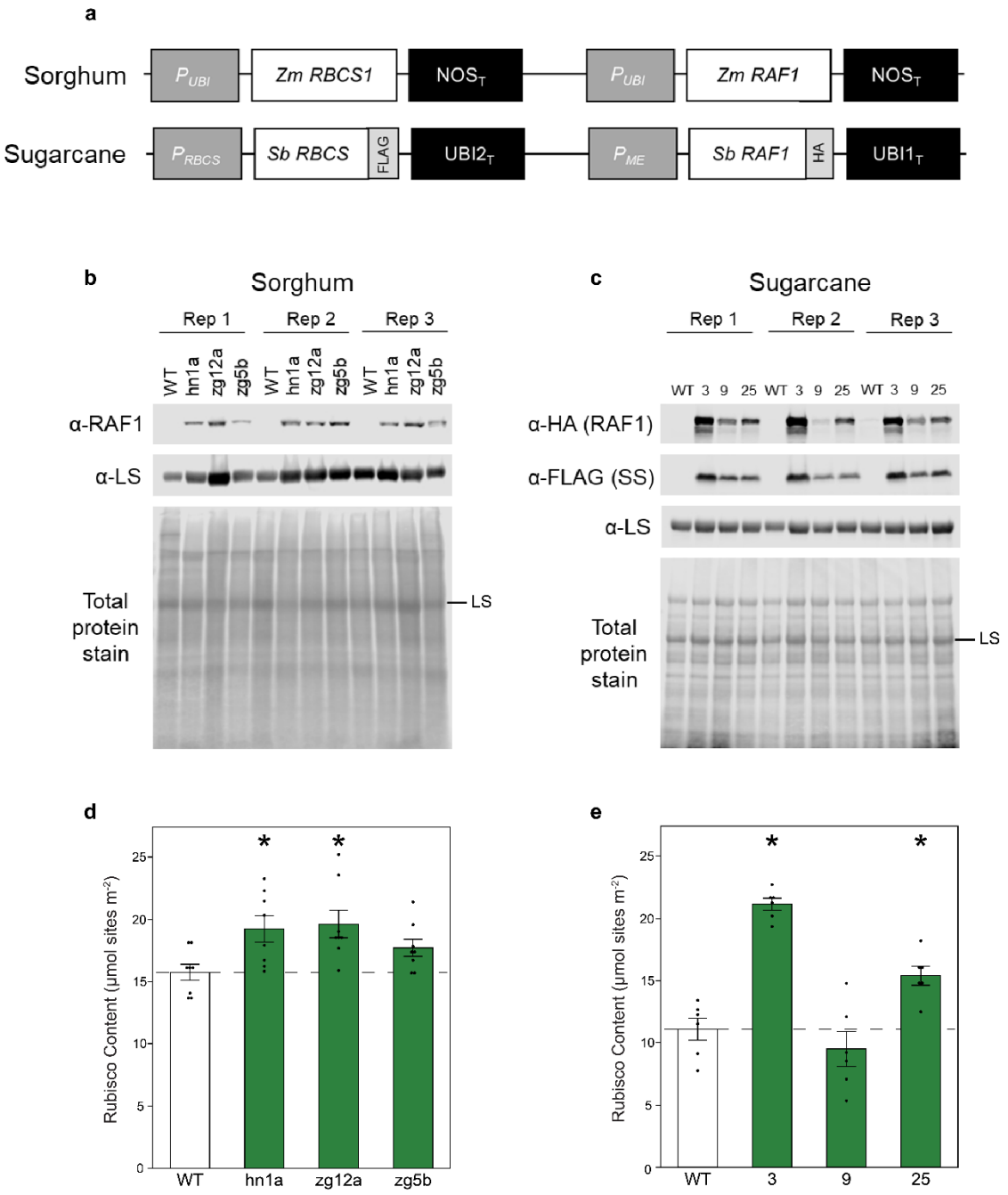

Fig. 1: Sorghum and sugarcane transformation constructs, protein expression and analysis of Rubisco content.

(a) Transgenes designed to upregulate Rubisco small subunit (*RbcS*) and Rubisco accumulation factor 1 (*Raf1*). The transgenes were stably transformed into sorghum (top) and sugarcane (bottom). The sugarcane construct contains FLAG and HA epitope tags. P, promoter; T, terminator, Sb, *Sorghum bicolor*; Zm, *Zea mays*; UBI, ubiquitin; NOS, nopaline synthase; ME, NADP-malic enzyme; HA, hemagglutinin. **(b)** Total soluble protein isolated on a leaf area basis from sorghum and **(c)** sugarcane, and analyzed by immunoblot. Three replicate plants (Rep) of each of the three transgenic events and of the wild-type (WT) control were probed with antibodies indicated to the left. -LS marks the Rubisco large subunit band. **(d)** Average Rubisco content per unit leaf area quantified by ^{14}C-CABP

binding in 6-week-old sorghum (n=8), and **(e)** 9-week-old sugarcane (n=6) grown in the greenhouse. Values are shown as the mean ± SEM. Asterisks indicate significant differences between WT and the transgenic line (*P < 0.05); one-way ANOVA, Dunnett's post hoc test.

Co-upregulation of RBCS and RAF1 is correlated with increased $V_{c,max}$, CO_2 assimilation, and photosynthetic light induction in sorghum

A-C_i responses showed that upregulated RBCS and RAF1 significantly increased assimilation rates above a C_i of ~100 µmol mol $^{-1}$, but not below (Fig. 2a). Maximum *in vivo* Rubisco carboxylation rates ($V_{c,max}$) at 25 °C, estimated from the *A*-C_i response, were significantly increased by 12% in the transgenic lines (Fig 2c), while maximum PEPC carboxylation rates ($V_{p,max}$) though slightly higher than WT did not differ significantly (Table 1). *In vitro* $V_{c,max}$ rates were increased by ~40% in the transgenic lines (Fig. 2d). A_{sat} measured at the current atmospheric [CO_2] also showed significant increases in the transgenic lines (Fig. 2b). g_{sw} was similarly significantly increased but this cannot account for increases in A_{sat} because no differences in C_i were observed between genotypes (Table 1). The effective quantum yield of PSII (Φ_{PSII}), measured by modulated chlorophyll fluorescence, was increased by 12% in the transformed plants in parallel with CO_2 assimilation (Table 1). Rubisco activation state, the fraction of Rubisco active sites that are catalytically active and therefore contributing to carboxylation, was not significantly different between lines (Table 1).

To identify if increased Rubisco would be beneficial to the activation of photosynthesis on shade to sun transition, induction of *A* over the first 30 min of transfer to high-light (PPFD = 1800 µmol m^{-2} s^{-1}) was measured (Fig. 2e). CO_2 assimilation in the transgenic lines was significantly higher than WT after 3 minutes of illumination following dark acclimation (Table 1) and remained higher for the remaining 27 minutes of measurement (Fig. 2e). Induction curves, normalized to the average *A* value over the last 5 minutes of illumination (A_{max}) were used to assess the speed of photosynthetic activation (Fig. S4a). On average, the transgenics took 4 minutes to reach 50% maximum CO_2 assimilation rates (A_{max}), compared to 6 minutes for WT (Fig. 2f). The transgenics were significantly taller and had more leaves than WT in the greenhouse (Fig. S5). Seed from these plants was collected for the field trial.

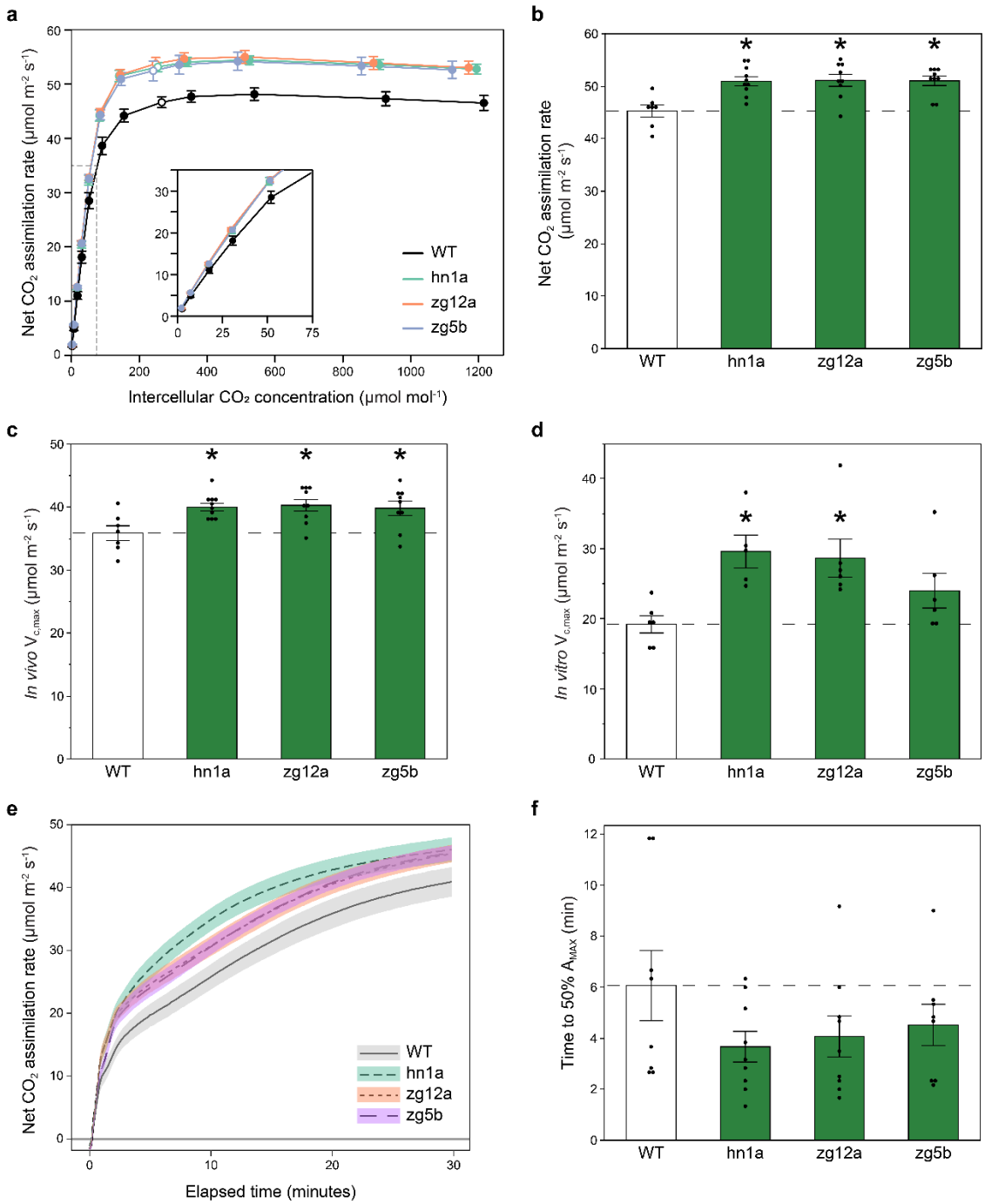

Fig 2: CO_2 response curves and photosynthetic induction to light of greenhouse grown sorghum plants.

(a) Response of light saturated CO_2 assimilation rates (A_{sat}) to intercellular [CO_2] (C_i). Measurements were made under the following conditions: light intensity of 1800 µmol m^{-2} s^{-1}, leaf temperature of 28 °C, and VPD 1.5 kPa. Measurement cuvette [CO_2] were varied from 10-1500 µmol mol^{-1} CO_2. Open points represent the measured value closest to the operating C_i (i.e the C_i where ambient CO_2 was 420 µmol mol^{-1}). **(b)** A_{sat} measured at 400 µmol mol^{-1} CO_2. **(c)** Maximum *in vivo* Rubisco carboxylation rate ($V_{c,max}$) at 25 °C estimated from response curves in panel **a** (n=7-10). **(d)** Maximum *in vitro* Rubisco carboxylation rate ($V_{c,max}$) at 25 °C (n=5-6). **(e)** Average CO_2 assimilation during the first 180 seconds of induction. **(f)** Time for A to reach 50% of A_{max}, where A_{max} is the average A from 25

212 to 30 minutes of illumination. Measurements were made on 5-week-old plants. Values are shown as the mean ±
213 SEM (n=7-10). Asterisks indicate significant differences between WT and the transgenic line (*P < 0.05); one-way
214 ANOVA, Dunnett's post hoc test.

215

216 **RBCS-RAF1 transgenic sorghum plants have increased photosynthesis and biomass under field**
217 **conditions**

218 A field trial in summer 2023 evaluated whether gains observed in the greenhouse could be
219 reproduced in a replicated field trial of 4-row plots. A randomized complete block design was
220 used with 6 replicate plots for each of the three RBCS-RAF1 transgenic events and WT (Fig. 4e;
221 Fig. S6a). A-C_i responses and light induction curves measured during the vegetative growth
222 stage were consistent with the greenhouse results. $V_{c,max}$, was again increased, with no
223 significant increase in the initial slope of the response, and light induction of A was faster (Fig
224 3a,b). These increases were also observed at boot stage but were absent during grain-filling
225 (Fig. 3c,d). Bundle sheath leakiness (Φ), the rate that CO_2 not fixed by Rubisco leaks from
226 bundle sheath back to mesophyll, was measured by combining gas exchange with carbon
227 isotope discrimination during the vegetative growth stage. In concert with increased $V_{c,max}$, Φ
228 was decreased by about 18% across all three transgenic lines, however these decreases were
229 not statistically significant (Fig. S7).

230 The field grown transgenic sorghum plants were also more vigorous than the WT, as evidenced
231 by a significant 15.5% increase in vegetative dry biomass at harvest (Fig. 4a). However, there
232 was no increase in seed biomass, which corresponded to a significant decrease in harvest index
233 (seed mass/total plant mass) compared to the WT (Fig. 4b-c). Seed composition was analyzed
234 using NIR and showed increased protein and decreased starch content in the transgenic lines,
235 with no change in fat or ash content (Fig. 4d). Number of panicles per plot, 100 seed weight and
236 average seed weight per panicle did not show any clear trends, however panicle emergence
237 was delayed by 3 to 6 days in the transgenic plants (Table S2). Leaf mass, chlorophyll content, N
238 and C contents, on a leaf area basis, did not differ between the WT and transgenic plants (Table
239 S3).

240

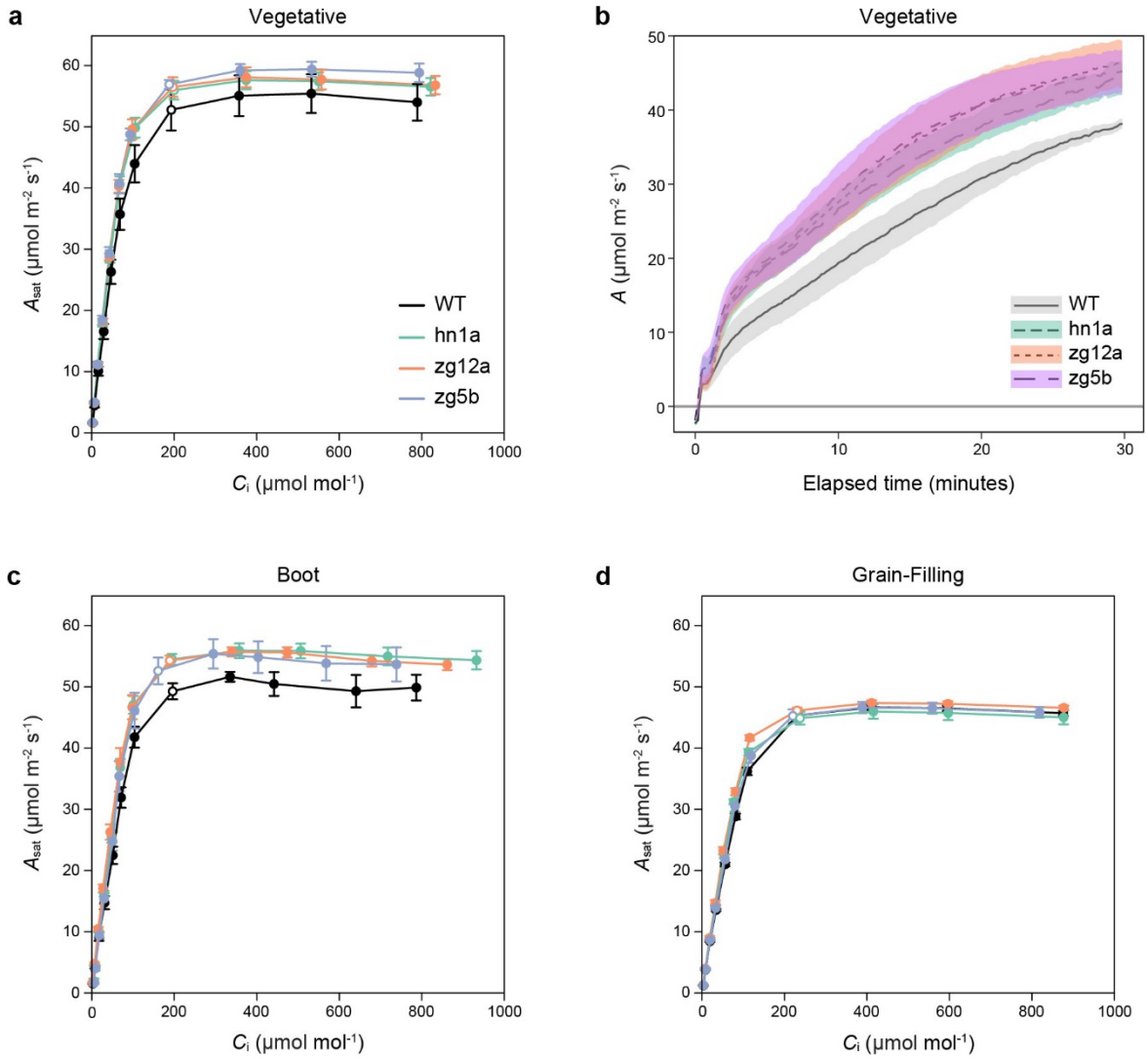

Fig. 3: CO_2 response curves and photosynthetic induction to light of field grown sorghum plants.

(a) Response of light-saturated CO_2 assimilation rates (A_{sat}) to intercellular [CO_2] (C_i) and **(b)** induction of A during the first 30 min of illumination at PPFD 1800 µmol m^{-2} s^{-1} of sorghum plants in the vegetative growth stage. **(c)** A_{sat} - C_i response of sorghum plants in the boot and **(d)** grain-filling growth stages. Open symbols on each curve show the measured value closest to the operating C_i (where ambient CO_2 is 420 µmol mol^{-1}). Values are shown as the mean ± SEM (n=4-6).

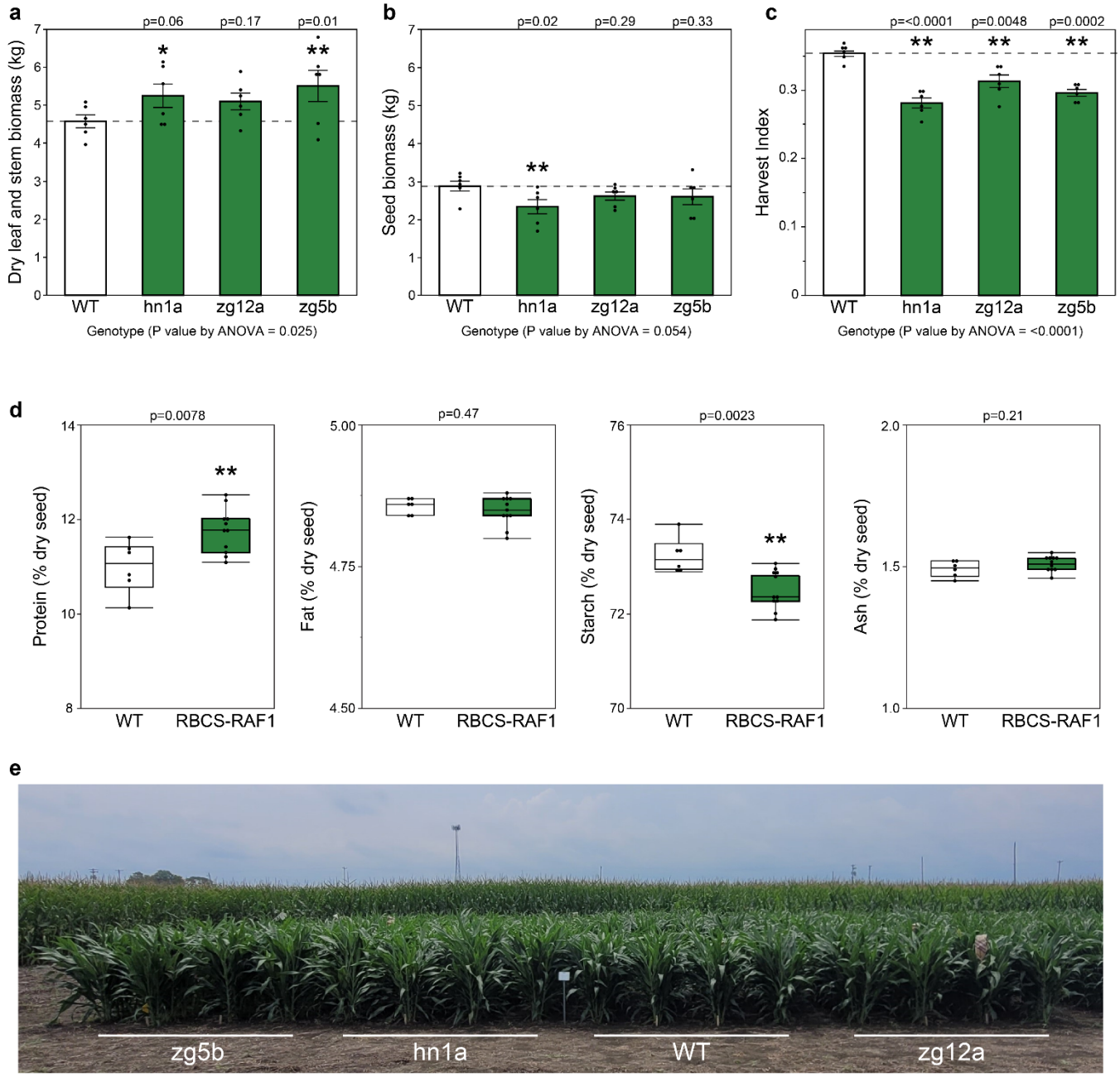

Fig. 4: Plant growth traits in field grown sorghum plants.

(**a**) Average dry leaf and stem biomass per plot and **(b)** average seed biomass per plot from field grown sorghum plants. **(c)** Harvest index (seed mass/total shoot mass) per plot. Values are shown as the mean ± SEM (n=6 plots). Asterisks indicate significant differences between WT and the transgenic line (**P < 0.05, *P < 0.1); one-way ANOVA, Dunnett's post hoc test. P values above each bar from Dunnett's post hoc test. **(d)** Percent protein, fat, starch and ash content of whole dry sorghum seeds (WT n= 6 plots, RBCS-RAF1 n=11 plots). **P < 0.05; pooled t-test. **(e)** Side view of 4 of the 24 four-row plots of the four sorghum genotypes tested at boot stage in the field in Urbana, Illinois summer 2023 (see Fig. S4a for full experimental design).

259

260 **Co-upregulation of RBCS and RAF1 in sugarcane increases photosynthetic efficiency and plant**
261 **productivity**

262 Measurements were made on 8-week-old greenhouse grown sugarcane plants. As in sorghum,
263 A-C_i responses showed significant increases in *in vivo* Rubisco activity ($V_{c,max}$) with no significant
264 change in the initial slope ($V_{p,max}$, Fig. 5a,d; Table 1). Similarly, A_{sat} and *in vitro* $V_{c,max}$ were
265 significantly increased at ambient atmospheric [CO_2] in the transgenics (Fig. 5c,e). There were
266 no significant differences in Rubisco activation state, g_{sw} or C_i: however, there was a marginal
267 increase in Φ_{PSII} in events 3 and 25 (Table 1). Assimilation of CO_2 was greater over the 30
268 minute light induction, in events 3 and 25, but not event 9 potentially due to a pleotropic effect
269 related to the location of the transgene insertion into the genome (Fig. 5b, Fig. S8).

270 Transgenic events 3 and 25 showed significant increases in main stem, and tiller and leaf dry
271 mass, amounting to total shoot dry mass increases of 37% and 81% respectively, but with no
272 increase in event 9 (Fig. 5f-h). Significant increases in plant height, stem width and leaf number
273 were also observed in events 3 and 25 compared to WT (Fig. S9). Leaf chlorophyll and mass per
274 unit area did not differ between genotypes (Table S3).

275

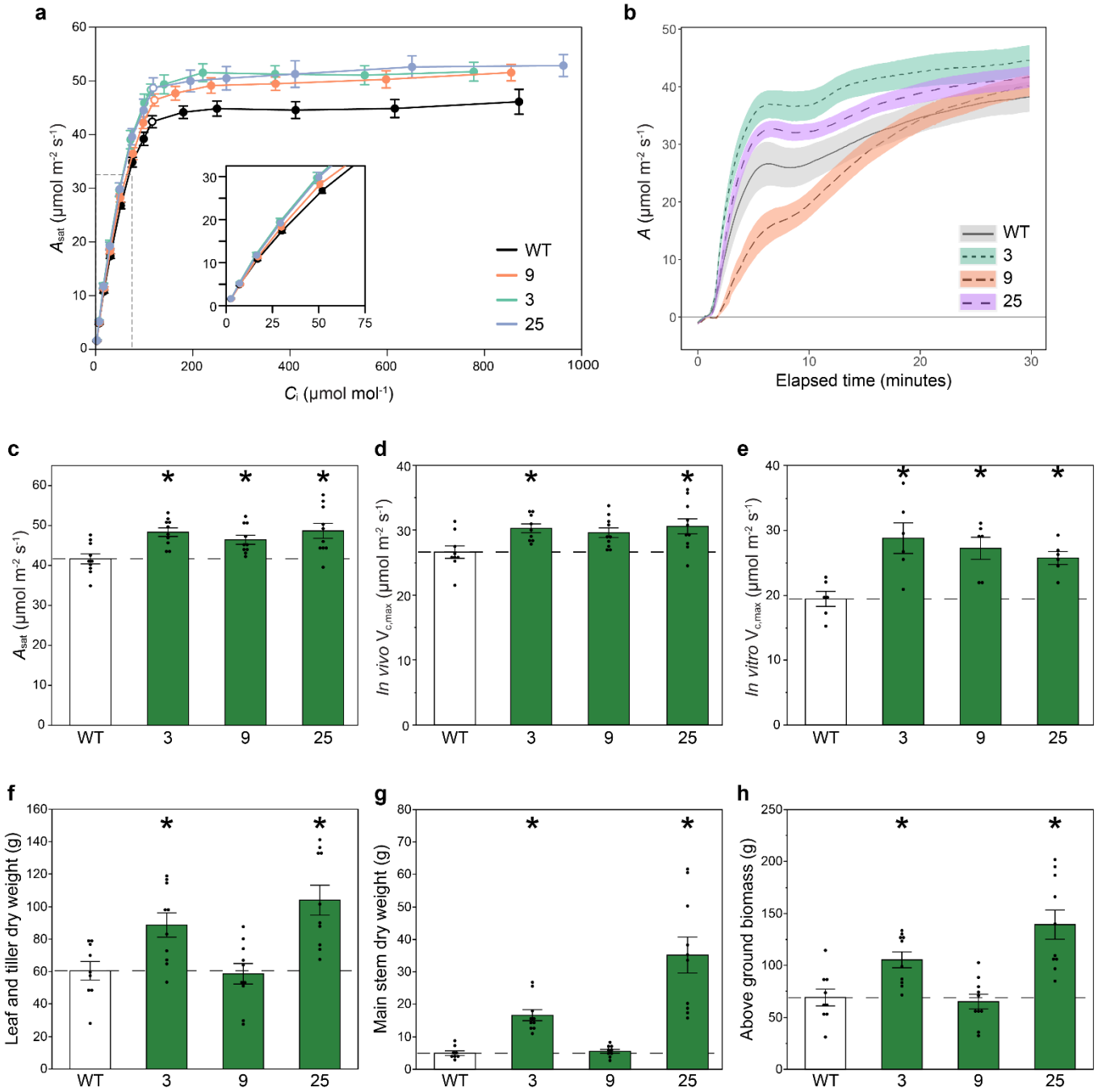

Fig 5: CO_2 response curves and plant growth traits of greenhouse grown sugarcane plants.

(a) Response of light-saturated CO_2 assimilation rates (A_{sat}) to intercellular [CO_2] (C_i). Measurements were at light intensity of 1800 µmol m^{-2} s^{-1}, leaf temperature 30 °C, and 65% humidity. Measurement cuvette [CO_2] was varied from 10-1500 µmol mol^{-1}. Open symbols show the measured value closest to the operating C_i (where ambient [CO_2] was 420 µmol mol^{-1}). **(b)** Induction of *A* during the first 30 min of illumination at PPFD 1800 µmol m^{-2} s^{-1}. **(c)** A_{sat} at 450 µmol mol^{-1} CO_2 **from panel a. (d)** Maximum Rubisco carboxylation rate *in vivo* ($V_{c,max}$) at 25 °C estimated from response curves in panel **a** (n=8-10). **(e)** Maximum *in vitro* Rubisco carboxylation rate ($V_{c,max}$) at 25 °C (n=6). **(f)** Leaf and tiller, **(g)** main stem, and **(h)** above ground total dry biomass of greenhouse grown sugarcane plants.

285 Values are shown as the mean ± SEM (n=8-10). Asterisks indicate significant differences between WT and the
286 transgenic lines (*P < 0.05); one-way ANOVA, Dunnett's post hoc test.

287

288 **Discussion**

289 Theoretical and experimental analyses have long suggested Rubisco to be the major limitation
290 of light-saturated photosynthesis in both C_3 and C_4 species (7, 18-20, 28). Consistent with this
291 hypothesis, transgenic upregulation of Rubisco content significantly increased Rubisco
292 carboxylation rates (V_{cmax}) and light-saturated leaf CO_2 assimilation rates (A_{sat}) in both sorghum
293 and sugarcane (Fig. 1 d-e, 2a-d, 3a-c, and 5a, c-e). Although Rubisco or electron transport can
294 limit assimilation in the plateau of a C_4 A-C_i curve (7, 29), the agreement between *in vivo* and *in*
295 *vitro* V_{cmax} estimates is consistent with primarily Rubisco-limited assimilation at high light (Fig.
296 2a,c-d and 5 a, d-e). The speed of light induction of CO_2 assimilation was also increased (Fig. 2e-
297 f and 3b). This has critical importance to increasing photosynthetic efficiency under the
298 fluctuating light conditions of crop canopies in the field (30, 31). Also consistent with limitation
299 by Rubisco, bundle sheath leakiness was decreased, although not significantly (Fig. S7). Finally,
300 and in concert with these increases in photosynthetic efficiency, a field trial of sorghum and a
301 greenhouse trial of sugarcane showed significant increases in productivity relative to the wild-
302 type from which the transgenics were derived (Figs. 4 and 5).

303 Rubisco is, by far, the most abundant single protein in leaves, constituting up to 50% of soluble
304 protein in C_3 plants and 20-30% in C_4 (32). These high amounts are attributed to the need to
305 offset the exceptionally low catalytic rate of carboxylation (k_{cat}) of Rubisco relative to other
306 enzymes. Its low k_{cat} is in turn considered in part a consequence of high specificity for CO_2
307 relative to the alternative substrate of O_2 (33). Sage & McKown (34) noted the much lower
308 available tissue volume that could house Rubisco in C_4 leaves, where it is functionally confined
309 to the bundle sheath, suggesting this as a constraint. This is less than half the volume available
310 in C_3 leaves. However, 3D microscopic analysis of the bundle sheath chloroplast stromal volume
311 in *Miscanthus* x *giganteus* suggested capacity for a doubling of actual Rubisco content (35).
312 *Miscanthus* is closely related to sorghum and sugarcane, and within the same subtribe,
313 Saccharinae (36). This observation is consistent with the observed increases in Rubisco content
314 of 25% in sorghum and up to 90% in sugarcane (Fig. 1d-e). The much higher level in sugarcane
315 may reflect that this was achieved by biolistic transformation, which could have resulted in
316 multiple insertions of the transgenes, while the three sorghum events were single insertion
317 events.

318 Given that increased Rubisco production is possible and beneficial, why have natural selection
319 and breeding not achieved this? One explanation is that Rubisco might only have become a
320 limitation very recently, due to rising atmospheric [CO_2]. On March 16, 2024, atmospheric [CO_2]

321 was recorded at 428 µmol mol^{-1} (21), which is almost double the average atmospheric [CO_2] of
322 the past 40,000 years (22, 37). Theory suggests that under the conditions in which our crop
323 ancestors evolved, Rubisco would not be a limitation and therefore selection pressure would
324 have been lacking, with the result that there may be little genetic variation for natural or
325 breeder selection as [CO_2] rises. Indeed given the large nitrogen cost of Rubisco, historically,
326 selection pressure was likely against any increase. It should be noted that half of the increase in
327 [CO_2] has occurred in the last 50 years, with [CO_2] rising from 323 µmol mol^{-1} to 428 µmol mol^{-1}
328 between 1974 and 2024 (21). By reference to the open symbols in Fig. 3, it is seen that at
329 today's atmospheric [CO_2] A_{sat} in the field-grown sorghum is controlled by the plateau of the *A*-
330 C_i response, i.e. predominantly by Rubisco activity. However, if it is assumed that C_i/C_a has been
331 conserved, then at the atmospheric [CO_2] in 1974, C_i would equal 129 µmol mol^{-1}. By reference
332 to Fig. 3, A_{sat} would then be mostly controlled by the initial slope of the *A*-C_i response, i.e. PEP
333 carboxylase activity ($V_{p,max}$), and insensitive to increase in Rubisco activity. The period in which
334 Rubisco has become limiting is therefore very short in terms of reproductive cycles. As
335 atmospheric [CO_2] continues to rise, Rubisco limitations will increase, and elevation of Rubisco
336 will be an important means to contribute toward future-proofing and advancing C_4 crop
337 productivity. An increase in A_{sat} was achieved here by only upregulating expression of *RbcS* and
338 *Raf1,* which infers three factors important for future manipulations. First, for Rubisco to be
339 increased, both the large (LS) and small (SS) subunits must be increased. That only upregulation
340 of *RbcS* was needed, is consistent with the observations that in tobacco *rbcL* is subject to
341 assembly-dependent translational regulation, and so controlled by the supply of SS (38) or in
342 rice the supply of SS upregulates *rbcL* transcript levels (39). Further studies are required to
343 determine which mechanism is occurring in sorghum and sugarcane. Second, although all three
344 transgenic sugarcane events showed expression of the *Sb* SS protein, in event 9 this did not
345 translate into improved productivity (Fig. 1c-e and 5f-h). Expression of *Sb* RAF1 was lowest in
346 this line, suggesting the importance of effective expression of RAF1 with SS (Fig.1c). Third, there
347 must either be 1) over-capacity in the C_4 cycle, 2) the C_4 cycle increases capacity in concert with
348 increased Rubisco activity, or 3) both occur. The fact that bundle sheath leakiness of CO_2
349 decreased and $V_{p,max}$ slightly increased with increased Rubisco is consistent with hypothesis 3
350 (24).

351 Similar to results reported in maize (26), increases in Rubisco content corresponded to
352 increases in Rubisco enzyme activity, resulting in higher photosynthetic rates and larger
353 biomass. Activation of Rubisco requires the chaperone protein Rubisco activase (RCA). In
354 contrast to previous studies in maize and rice (26, 40), no decrease in the fraction of active
355 Rubisco was observed in the transgenic plants, indicating that sorghum and sugarcane must
356 have had sufficient RCA to support the activation of all their additional Rubisco (Table 1). In
357 these previous studies, increased Rubisco content was achieved by overexpressing endogenous
358 *RbcS* with or without *Raf1*. Here, *RbcS* and *Raf1* genes from maize and sorghum were expressed
359 in sorghum and sugarcane respectively, so the transgenic plants are assembling some chimeric

360 Rubiscos comprised of the foreign transgenic SS and endogenous LS. Maize, sorghum and
361 sugarcane have been reported to have very similar k_{cat} (41, 42), implying that the increases in
362 Rubisco activity reported here are solely due to increased Rubisco active sites and not changes
363 in Rubisco kinetic properties. In addition, the FLAG tag fused to *RbcS* in the sugarcane construct
364 did not appear to interfere with Rubisco activity (Fig. 5e).

365 In dense modern crop canopies, only the uppermost leaves might experience light saturated
366 conditions. Most leaves will experience frequent light fluctuations, or sunflecking, due to the
367 passage of clouds, shadowing by overlying leaves as solar angle changes and wind driven
368 movements (30, 31). The speed with which photosynthetic efficiency can adjust to light
369 fluctuations has been shown to have a profound effect on whole crop daily CO_2 assimilation
370 and productivity (43, 44). A key factor here is the speed of induction of *A* on transfer of a leaf
371 from shade to sun. Modeling and experimental studies have shown the speed at which Rubisco
372 activity increases to be critical to induction in both C_3 and C_4 crops (23, 45, 46). Here, increased
373 Rubisco content coincided with more total CO_2 assimilation over the 30 minutes of induction in
374 all three sorghum events and two of the sugarcane events (Fig. 2e, 3b, 5b). Speed of induction,
375 measured as time to 50% A_{max}, was also increased in the transgenic sorghum lines but not in
376 sugarcane (Fig. 2f and Table 1). This is consistent with computational results from Wang *et al.*
377 (2021), which suggest that Rubisco activation is the main limiting factor in the speed of
378 photosynthetic induction in sorghum, while the speed of stomatal opening and the
379 concentration of the PPDK regulatory protein exert more control in sugarcane.

380 In the greenhouse, significant increases in growth of both sorghum and sugarcane were
381 observed at an individual plant level (Fig. 5f-h; Fig. S5). Importantly, and consistent with
382 increased CO_2 assimilation rates during vegetative and boot stages, leaf and stem biomass was
383 significantly increased by an average of 15.5% in the RBCS-RAF1 sorghum field plots relative to
384 the WT controls, a desired characteristic for C_4 biomass crops (Fig. 4a). However, grain yield per
385 plot did not increase, due to a significant decrease in harvest index (Fig.4c). Although sorghum
386 cultivar RTx430 has become the standard for transformation and experimental analyses, it is a
387 40-year old inbred line (47-49) and might be sink-limited. There is similar evidence for sink
388 limitations in a 25-year old hybrid cultivar; when sorghum was grown under well-watered
389 conditions under open-air CO_2 enrichment using FACE technology, photosynthetic capacity and
390 photosynthetic rates were increased (50-52). Yet, as in our experiment, stover increased while
391 harvest index declined by 7% (53). Sink limitation at grain filling results in accumulation of non-
392 structural carbohydrates in the source tissues, causing down-regulation of photosynthetic
393 genes, notably *RbcS* (54). The loss of *in vivo* Rubisco activity ($V_{c,max}$) during grain filling evident in
394 Fig. 3d is consistent with sink limitation. Alternatively, grain yields may not have increased due
395 to alternative factors such as delayed panicle emergence or decreased transgene expression. It
396 is also important to note that Rubisco levels increased without an associated change in total
397 soluble protein, LMA or leaf N content (Fig. 1 and Table S3). This suggests that more leaf N Is

398 invested into Rubisco in the transgenic plants and therefore less N allocated to other leaf
399 proteins. Although there was no negative impact on photosynthesis, altered N use may affect
400 other processes including grain filling. Testing whether greater grain yields can be obtained will
401 require the production of hybrids and/or transformation of current elite cultivars. Upregulation
402 of Rubisco has been achieved here, as a test of the concept that more Rubisco would translate
403 to more efficient photosynthesis and productivity in today's atmosphere, by addition of extra
404 copies of *RbcS* and *Raf1*. Alternatively, a future approach for upregulating Rubisco could be
405 using DNA editing to mutate repressive elements in the promoter regions of the native *RbcS*
406 and *Raf1* genes.

407 Despite significant breeding efforts, the average yield of sorghum has not changed over 30
408 years, nor has the yield of sugarcane in the USA in the last 20 years (Fig. S10a,b). This might
409 reflect increasingly adverse weather conditions. However, even in the USA where it might be
410 assumed that favorable agronomy would allow the yield potential to be realized, there is little
411 evidence of yield improvement since 1991, even in the most favorable years (Fig. S10a).
412 Therefore, if the photosynthetic and productivity improvements found here by upregulating
413 Rubisco translate into parallel yield improvements in elite cultivars and hybrids, this could be
414 very useful for integration into breeding programs. This successful test-of-concept suggests
415 multi-location and/or multi-year replicated yield trials of Rubisco upregulation in elite material
416 as the next proving step. Given the great value and global significance of this key economic
417 clade of crops both for food and biomass, the results here indicate an important opportunity to
418 achieve increased productivity under rising atmospheric [CO_2].

419

420 **Methods**

421 **Sorghum plasmid assembly and transformation**

422 A 3.6 kb fragment containing the *Raf1* expression cassette regulated by the maize ubiquitin
423 promoter was isolated from the plasmid pPTN1063 (26) by digesting the vector with *Kpn*I and
424 *Hind*III. The fragment was then blunted with T4 DNA polymerase. Plasmid pPTN438 (38)
425 (containing the *RbcS* expression cassette) was linearized via *Kpn*I digestion and blunted with T4
426 DNA polymerase. The pPTN1063 fragment and linearized pPTN438 plasmid were then ligated
427 resulting in the final binary vector pPTN1589. Sorghum inbred RTx430 was transformed with
428 pPTN1589 using agrobacterium as previously described (55).

429

430 **Sugarcane plasmid assembly**

431 Recombinant DNA constructs were assembled with Golden Gate cloning to highly express
432 Rubisco small subunit (*RbcS*) and Rubisco accumulation factor 1 (*Raf1*) from *Sorghum bicolor* in

433 sugarcane. The open reading frame (ORF) of *SbRbcS* (Sobic.005G042000) and ORF of *SbRaf1*
434 (Sobic.006G269400) were synthesized with 1X FLAG tag and 6X HA tag, respectively (GenScript,
435 Piscataway, NJ). *SbRbcS*-FLAG was subcloned under transcriptional control of the maize RBCS
436 promoter + 5'UTR and the *Panicum virgatum* UBI2 (PvUBI2) terminator. The synthesized
437 *SbRaf1*-HA was subcloned under transcriptional control of the maize NADP-ME promoter and
438 *Panicum virgatum* UBI1 (PvUBI1) terminator. The selectable marker gene *npt*II was subcloned
439 under transcriptional control of the ubiquitin promoter from *Zea mays* and SbHSP16.9
440 terminator from *Sorghum bicolor*. The three expression cassettes were subcloned into a L2
441 construct downstream of an RB7 matrix attachment region (MAR) and upstream of TM2 MAR
442 from *Nicotiana tabacum* serving as insulators and confirmed by Sanger sequencing. The
443 minimal expression construct flanked by MARs was excised from the plasmid backbone using
444 the *I-Sce*1 restriction enzyme and gel purified prior to biolistic transformation into sugarcane.

445

446 **Sorghum transgene copy number analysis**

447 Transgene copy number was measured using digital droplet PCR (ddPCR) following the
448 protocols from Głowacka et al. (56), with slight modifications. See Table S1 for primers used
449 (57). Sorghum genomic DNA was digested overnight with HindIII. A 20 µL ddPCR reaction mix
450 contained 20 ng of the digested DNA, 10 µL QX200 ddPCR EvaGreen Supermix (186-4034,
451 BioRad, Hercules, CA) and primers at a final concentration of 100 nM. Droplets were generated
452 using a QX200 droplet generator (186-4002, Bio-Rad) by combining 20 µL of the reaction mix
453 with 70 µL of EvaGreen droplet generation oil (186-4005, Bio-Rad). The PCR reaction was
454 conducted in a deep-well thermal cycler (C1000 Touch, 185-1196, Bio-Rad) with the following
455 conditions: 95 °C for 5 minutes, 40 cycles of 95 °C for 30 seconds and 59 °C for 1 minute, then 4
456 °C for 5 minutes and 90 °C for 5 minutes, with a ramp rate of 2.5 °C/second at each step.
457 Immediately after the PCR, measurements were taken using a QX200 droplet reader (186-4003,
458 Bio-Rad).

459

460 **Generation and PCR confirmation of transgenic sugarcane plants**

461 The linearized, minimal construct containing *SbRbcS*, *SbRaf1* and NPTII cassettes flanked by
462 matrix attachment regions was introduced into sugarcane cv. CPCL02-0926 by biolistic gene
463 transfer as described previously (58). Briefly, cross-sections of sugarcane leaf whorls above the
464 shoot apical meristem were cultured on a modified Murashige & Skoog medium (MS) with B5
465 vitamins (PhytoTech Labs, KS, USA) supplemented with 3 mg/L of 2,4-Dichloro phenoxy acetic
466 acid (PhytoTech Labs) and maintained at 28 ℃ in the dark for induction of embryogenic callus.
467 For biolistic gene transfer, the minimal expression cassette was coated onto gold particles and
468 introduced into embryogenic calli using biolistic PDS-1000/He delivery system (Bio-Rad) as
469 described previously (59). Following 4 weeks of selection of transformed calli on the medium
470 containing the antibiotic Geneticin®, calli were sub-cultured onto regeneration media (MS

media with B5 vitamins, supplemented with 1.86 mg/L of α-Naphthaleneacetic acid/NAA (PhytoTech Labs) and 0.09 mg/L of 6-Benzylaminopurine/BAP (PhytoTech Labs)) and maintained at 28 ℃ incubator with 16/8 hr light (100 µmol m^{-2} s^{-1}) and dark cycle. Regenerated shoots were transferred to modified MS basal medium (PhytoTech Labs) for shoot elongation and rooting. Rooted plantlets were transferred to soil and acclimatized in a temperature-controlled growth chamber maintained at 28 ℃ day and 22 ℃ night temperature with 16/8 hr light (400 µmol m^{-2} s^{-1}) and dark cycle for growth and further analysis.

For the PCR confirmation of transgenic events, DNA was isolated from 100 mg of leaf tissues using CTAB method with modifications (60). PCR reactions were performed on a thermocycler (Applied Biosystems, Foster City, CA) using standard Taq buffer, dNTPs and hot start Taq polymerase (New England Biolabs Inc, Ipswich, MA). See Table S1 for primers used for PCR amplification. Amplicons were resolved with electrophoresis on a 1.2% agarose gel and visualized under UV transilluminator (Bio-Rad).

Plant growth – greenhouse conditions

T2 homozygous *Sorghum bicolor* (inbred RTx430) seeds from 3 independent single insertion events and non-transformed WT seeds from the same harvest date were sowed into plastic potting trays 6 cm x 6 cm x 5.4 cm deep, filled with BM7 growing medium (BM7 All-Purpose Bark Mix, Berger). After about 14 days seedlings were transplanted into 9.5L plastic pots filled with BM7 growing medium supplemented with 44 cm^3 of 13-13-13 (N-P-K) granulated slow-release fertilizer (Osmocote, ICL-Growing Solutions). Sugarcane (*Saccharum officinarum* cv. CPCL02-0926) plantlets clonally propagated from three independent T0 transformation events and non-transformed WT plants were also grown in the greenhouse. Single node segments from mature stalks were transplanted into 9.5L plastic pots filled with BM7 growing medium supplemented with 44 cm^3 of 13-13-13 (N-P-K) granulated slow-release fertilizer. Both sorghum and sugarcane were grown under natural illumination (Figure S11). Lights turned on from 6:30am to 9:30pm (15 hour days), providing an additional 350 to 450 µmol $m^{-2}s^{-1}$ of LED light, and turned off when outside light intensity surpassed 350 watts/m^2 (~800 µmol $m^{-2}s^{-1}$). The greenhouse temperature was kept between 25-28°C in the day and 24-26 °C at night. Both sorghum and sugarcane plants were fertilized with a rotation of 20-10-20 & 15-5-15 liquid fertilizer (JR Peters INC) at 300 ppm N twice a week. Once a month a $MgSO_4$ (100 ppm) and iron (10 ppm) drench was applied (Sprint 138, BASF Corporation).

Sugarcane plants were harvested after 2 months of growth. Immediately prior to harvesting, leaf number (fully expanded), tiller number, plant height and stem width were measured. Stem width was measured at the widest point approximately 5 cm above the soil using calipers. Height was measured from the soil to the top of the youngest fully expanded leaf (leaf collar present). Leaf mass per area (LMA) was measured from 3.15 cm^2 of leaf discs, which were dried until constant weight and weight recorded. Chlorophyll content was measured using a SPAD

meter (502, Spectrum Technologies). Harvested material was partitioned into main stem biomass and leaf plus tiller biomass and dried at 60°C to steady state weight. Above ground biomass was calculated as the sum of stem, leaf and tiller biomass.

Plant growth – field conditions

Sorghum seed obtained from the plants in the greenhouse experiment were harvested and used for a field experiment. A randomized complete block design with six blocks was used. Each block contained 16 rows in a North-South direction, made up of four row plots from each of the transgenic lines and WT control (Fig. S6a). Prior to planting the ground was worked with a field cultivator (April 27 2023), and no fertilizer was applied to the soil. Seeds were sowed using a precision planter at a density of 8.6 m^{-2} (Almaco) on June 2nd 2023 on the Crop Sciences Farm of the University of Illinois SoyFACE Experimental Station (40°02'36.0"N 88°13'48.5"W). Weather data was collected with an automatic weather station on the Farm (Fig. S6b-d). July 5th Warrior II with Zeon technology (Syngenta) was applied at a moderate rate of 0.07 dm^3/ha for the control of flea beetles. August 2nd Mustang Maxx (FMC Corporation) was applied at moderate rate of 0.1 dm^3/ha for the control of aphids.

To avoid any release of pollen, paper bags enclosed the panicles, sealed at the peduncle, prior to anthesis, and remaining until harvest (recorded as panicle emergence date). Plants were harvested by hand on October 4th from the middle two rows of each plot by cutting stems at ground level. Two plants from either end of each row were discarded to avoid edge effects. Harvested material was partitioned into stem/leaves and panicles with seed. Stem and leaves were dried to a constant weight in custom made drying ovens at 60°C and panicles with seed were dried at 30°C. Dry weights per plot were obtained for both, then seed was collected using a threshing machine (BT 14-E Belt Thresher, Almaco). The machine was cleaned between each sample to avoid contamination. Total seed weight per plot, and 100 seed weights were then determined. Above ground biomass was calculated as the sum of stem, leaf, panicle and seed biomass. Harvest index was calculated as seed biomass divided by total above ground biomass. Seed weight per panicle was estimated by dividing seed weight per plot by panicle number per plot. Seed protein, starch, fat and ash content were estimated on a percent basis using a near-infrared reflectance (NIR) analyzer (DA 7250, Perten Instruments). Seeds were placed into the sample dish and analyzed using a built in program for whole-seed evaluation ("Sorghum-Grain"). Chlorophyll content was measured using a SPAD meter (502, Spectrum Technologies) on August 30th. LMA was measured from from 6.06 cm^2 of leaf tissue collected August 31st.

Transcript and protein expression

Prior to RNA and protein extraction tissue was disrupted and homogenized as described previously (61). RNA was extracted from 1.9 cm^2 of leaf tissue from the youngest fully

546 expanded leaf of greenhouse and field-grown sorghum, using the NucleoSpin RNA Plant Kit
547 (Macherey-Nagel). 700 µL of the lysis buffer was used. RNA quantity and quality was assessed
548 using a NanoDrop (Thermo Fisher Scientific). cDNA was synthesized with Superscript IV VILO
549 Mastermix with ezDNase (Thermo Fisher Scientific). qPCR, primer design and validation were
550 conducted as described in Salesse-Smith et al 2024 (61), with the exception that an anneal
551 temperature of 60°C was used for all primer sets. See Table S1 for primer sequences. Primer
552 efficiencies were between 100-105%. Calibrated Normalized Relative Quantities (CNRQ) were
553 calculated using qBase+ software v.3.2 (CellCarta) based on the expression of two reference
554 genes, SbEIF4α and SbActin11.

555 Total protein was extracted from 1.9 cm^2 of leaf tissue from the youngest fully expanded leaf of
556 greenhouse-grown sorghum and sugarcane and field-grown sorghum. Protein extraction and
557 western blots were performed as described previously (61). The following primary antibodies
558 were used: anti-HA (AS12 2220, Agrisera) at a 1:5000 dilution, anti-LS (AS03 037, Agrisera) at a
559 1:10000 dilution, anti-FLAG (F7425-.2MG, Sigma-Aldrich) at a 1:5000 dilution and anti-RAF1
560 (custom rabbit antibody, Pacific Immunology) at a 1:1000 dilution. For the custom antibody, a
561 23 amino acid immunograde peptide from the maize RAF1 protein (aa 211-233;
562 KGFPRWRGEEGWEAFSKDSPADC) was synthesized and antisera generated by Pacific
563 Immunology. Relative abundance of LS protein was estimated using Empiria Studio Software
564 version 3.2 (Li-COR, Biosciences).

565

566 **Rubisco content, activity and activation measurements**

567 Leaf discs were sampled from the youngest fully expanded leaves of greenhouse-grown
568 sorghum (1.9 cm^2) and sugarcane (2.5 cm^2) plants, snap-frozen in liquid nitrogen and stored at
569 -80°C. Samples were taken from the same location gas exchange measurements were made the
570 day after measurements were completed. Soluble protein was extracted in 2 mL of N_2-sparged
571 extraction buffer: 50 mM EPPS-NaOH pH 8, 1 mM EDTA, 5 mM $MgCl_2$, 1% (w/v) PVPP, 5 mM
572 DTT and 1% (v/v) protease inhibitor cocktail (P9599, Sigma-Aldrich). Frozen leaf discs were
573 ground in ice-cold Ten Broeck homogenizers (7 mL, Corning) containing extraction buffer. Total
574 soluble protein was quantified using the Qubit Protein Assay Kit (Q33211, Life Technologies) on
575 the Qubit 3 Fluorometer (Q33216; Life Technologies). Total Rubisco content was measured by
576 ^{14}C-CABP binding as previously described (Ruuska et al., 1998; Sharwood et al., 2008). 100 µL of
577 protein lysate was mixed with an equal volume of Rubisco activation buffer (50 mM EPPS-NaOH
578 pH 8, 1 mM EDTA, 20 mM $MgCl_2$, 30 mM $NaHCO_3$) and let sit at room temperature. After 20
579 minutes, 60 µM of ^{14}C-CABP was added to the mixture and left at room temperature for an
580 additional 30 minutes, and then transferred to ice. 100 µL of the activated Rubisco protein
581 mixture was loaded onto the size-exclusion chromatography columns and fractions containing
582 ^{14}C-CABP – Rubisco complexes collected. The amount of ^{14}C-CABP was determined by liquid
583 scintillation (Packard Tri-Carb 1900 TR, Canberra Packard Instruments Co). Leaf Rubisco
584 content was calculated as described previously (62).

585 Rubisco activity was determined at 25°C by incorporation of $^{14}CO_2$ into acid-stable products
586 (63). An extended protocol can be found online: dx.doi.org/10.17504/protocols.io.bf8cjrsw.
587 Sorghum (1.7 cm^2) and sugarcane (2.26 cm^2) were collected as indicated above. Soluble protein
588 was extracted in 2 mL of N_2-sparged extraction buffer: 50 mM Bicine-NaOH pH 8.2, 20 mM
589 $MgCl_2$, 1 mM EDTA, 2 mM benzamidine, 5 mM ε-aminocaproic acid, 50 mM 2-mercaptoethanol,
590 10 mM DTT, 1% (v/v) protease inhibitor cocktail, 1 mM phenylmethylsulphonyl fluoride, and 1%
591 (w/v) polyvinylpolypyrrolidone. Supernatant was immediately used to measure initial and total
592 Rubisco activity, with two technical replicates per measurement. Initial activity was measured
593 by adding 25 µl of protein lysate to assay buffer (100 mM Bicine-NaOH pH 8.2, 20 mM $MgCl_2$,
594 10 mM $NaH^{14}CO_3$ (18.5 kBq μmol^{-1}), 2 mM KH_2PO_4, and 0.6 mM RuBP). After 30 s reactions were
595 quenched with 100 µl of 10 M formic acid. For total activity measurements, RuBP was added 3
596 min after the protein lysate to allow for carbamylation of Rubisco and quenched after 30 s.
597 Reactions were dried at 100 °C, then the residue dissolved in 400 µl deionized water and added
598 to scintillation cocktail for acid-stable ^{14}C determination by liquid scintillation. Rubisco
599 activation state was calculated as initial/total activity.

600

601 **Leaf gas exchange measurements**

602 CO_2 response (A-C_i) and light induction curves were measured on the youngest fully expanded
603 leaves using an infrared gas exchange system LI-6800 fitted with the multiphase flash
604 fluorometer and 6 cm^2 cuvette (6800-01A, LI-COR Environmental). CO_2 response curves were
605 measured simultaneously with chlorophyll fluorescence and used to assess A, C_i, g_{sw}, ϕPSII,
606 $V_{c,max}$ and $V_{p,max}$. A-C_i curves were measured in the field-grown sorghum on July 10th, August 4th
607 and August 29th. Leaves were acclimated to the following conditions: light intensity of 1800
608 $\mu mol\ m^{-2}\ s^{-1}$, leaf temperature of 30 °C, CO_2 reference concentration of 400 $\mu mol\ mol^{-1}$ and 65%
609 humidity. Once A and g_{sw} stabilized, response curves were initiated using the following
610 sequence of reference CO_2 concentrations: 400, 300, 200, 120, 70, 30, 10, 400, 400, 500, 700,
611 900, 1200, and 1500 $\mu mol\ mol^{-1}$. Measurements were logged 3 to 5 minutes after each new CO_2
612 step. A-C_i curves for greenhouse-grown sorghum were measured under the same conditions
613 except for the following changes: a leaf temperature of 28 °C was used and the CO_2 sequence
614 used concentrations of 600 and 800 $\mu mol\ mol^{-1}$ CO_2 instead of 700 and 900. Sugarcane A-C_i
615 curves used a CO_2 reference concentration of 450 $\mu mol\ mol^{-1}$ and the following sequence of
616 CO_2: 450, 1500, 1250, 1000, 750, 600, 500, 400, 300, 200, 120, 70, 30, and 10 $\mu mol\ mol^{-1}$. $V_{c,max}$
617 and $V_{p,max}$ at 25°C were estimated using the *fit_c4_aci* function from the PhotoGEA R package
618 (64), which fits a mechanistic model to the measured CO_2 response curves (7). In this method,
619 values of $V_{c,max}$, $V_{p,max}$, and R_L are varied to find the best fit of the full equation for enzyme-
620 limited assimilation (Equation 4.21 of von Caemmerer 2000) to all points in each curve (29).

621 Light induction curves were used to assess average A in either the first 180 or 300 seconds since
622 the light was turned on and time to 50% A_{max}, which is determined from the normalized
623 induction curves. Leaves were acclimated to the following conditions: light intensity of 0 µmol

624 m^{-2} s^{-1}, leaf temperature of 28°C (greenhouse-grown sorghum) or 30 °C (field-grown sorghum
625 and sugarcane), CO_2 sample concentration of 400 (sorghum) or 450 µmol mol^{-1} (sugarcane) and
626 65% humidity. After 30 minutes in the dark, light was increased to 1800 µmol m^{-2} s^{-1} and data
627 points logged every 10 s over the course of 30 min. Average assimilation after 300 seconds of
628 light induction was calculated for sugarcane, while 180 seconds was used for sorghum due to
629 differences in each species overall speed of induction. After gas exchange measurements were
630 completed on the greenhouse-grown sorghum plants, leaf number, tiller number and height
631 were recorded.

632

633 **Estimating bundle sheath leakiness using carbon isotope discrimination coupled with leaf gas**
634 **exchange**

635 A LI-6800 gas exchange system (LI-COR Environmental) with the large light source chamber
636 (6800-03) was coupled to a tunable-diode laser absorption spectroscope (TDLAS model TGA
637 200A; Campbell Scientific) to measure online carbon isotope discrimination as described
638 previously (24). The TDL was connected to the LI-6800 reference air stream using the port on
639 the back of the sensor head, and connected to the sample air stream using the port on the
640 front of the sensor head. CO_2-free air (N_2/O_2) with 21% O_2 was created by mixing two gas
641 streams with mass flow controllers (OMEGA Engineering Inc.). This air supplied the gas
642 exchange system, and was used in the calibration to correct for any drift in the TDL during
643 measurements. The TDL was calibrated using a 2-point calibration where a linear fit is applied
644 using the measurements from two calibration tanks with known [$^{12}CO_2$], [$^{13}CO_2$] (NOAA Global
645 Monitoring Laboratory). The measurements cycled through four gas streams in the following
646 sequence: calibration points 1500 and 100 ppm CO_2 (NOAA Global Monitoring Laboratory), LI-
647 COR 6800 reference air stream, leaf chamber air stream, and reference air stream a second
648 time. Each step had a duration of 30 s, except for the leaf chamber air, which had a duration of
649 600 s for a total cycle time of 720 s. Measurements were averaged over the last 10 s to
650 produce a single data point for the calibration and reference measurements each cycle. For the
651 sample line, measurements were averaged over 10 s intervals, excluding the first 10 s, to have
652 59 data points each cycle.

653 The gas exchange system was set to the following conditions: light intensity of 0 µmol m^{-2} s^{-1},
654 leaf temperature of 27°C, flow rate of 300 µmol s^{-1}, 21% O_2, and 800 µmol mol^{-1} CO_2. Once
655 steady-state respiration was reached, five consecutive measurements were logged to measure
656 dark respiration. Afterwards the system was initiated to auto-log at 10 s intervals over the
657 course of 30 min. Light intensity increased to 1800 µmol m^{-2} s^{-1} upon initiation of the auto
658 program. Sorghum leaves from the field were cut from plants pre-dawn, submerged in water
659 and brought to the lab where they were re-cut underwater and left in the dark until measured.
660 Only steady state measurements of leakiness were calculated (25-30 min after light turned on).

Observed photosynthetic discrimination ($\Delta^{13}C$) was derived and bundle sheath leakiness (ϕ) was subsequently calculated from gas exchange parameters and $\Delta^{13}C$ as described previously (65, 66). Data processing and calculations of $\Delta^{13}C$ and ϕ were done using the MATLAB tool developed previously (24), with minor modifications to apply the 2-point calibration discussed above.

Carbon and nitrogen analysis

Leaf tissue from field grown sorghum was oven dried to a constant weight, ground and total carbon (C), C isotope analysis (δ15C), total nitrogen (N), and N isotope analysis (δ15N) measured using an elemental analyzer (Costech Elemental Combustion System 4010, Costech Analytical Technologies) coupled with a continuous flow isotope ratio mass spectrometer (DeltaV Advantage, Thermo Fisher Scientific). Spinach leaves (National Institute of Standards and technology Standard Reference Material 1570a) and acetanilide (USA Analytical) were used as standards for C and N analysis. Isotope analysis was measured relative to the international standards NBS 19 for C ($\delta^{13}C_{V\text{-}PDB}$ = 1.95‰) and atmospheric N_2 for N ($\delta^{15}N_{Air}$ = 0‰).

Statistical analysis

Normality of the data was tested with Shapiro-Wilk's test, and homoscedasticity with Brown-Forsythe's test. If criteria for normal distributions and equal variance was met one-way ANOVA followed by Dunnett's *post hoc* test for transgenic mean comparison against the WT control was performed. Data were considered significant at $P < 0.05$, and at $P < 0.1$ when specified. If criteria for normality was violated Wilcoxon's non-parametric test was applied. Analysis of field growth traits (Fig. 4, Table S2) was performed using a randomized block design with 6 blocks. Statistical tests used are indicated in each figure or table legend. Jmp pro version 17.0.0 software was used for all statistical analyses.

Acknowledgements

We thank Montgomery Flack for maintenance of the greenhouse plants. We thank David Drag, Ben Thompson, and Andy Wszalek for help with the maintenance of the sorghum field experiment and field harvest. We thank Edward Lochocki for assistance during field work and Samantha Stutz for maintenance of the TDL. We also thank Mike Masters and Chuck Hyde for performing the C and N analysis and Ben Haas for initial help with plasmid assembly. We are grateful to Dr. Berkley Walker for the kind gift of RuBP. This work was funded by the DOE Center for Advanced Bioenergy and Bioproducts Innovation (U.S. Department of Energy, Office of Science, Biological and Environmental Research Program under Award Number DE-SC0018420). Any opinions, findings, and conclusions or recommendations expressed in this

publication are those of the author(s) and do not necessarily reflect the views of the U.S. Department of Energy.

Conflict of Interest

The authors declare no conflicts of interest.

Author Contributions

CES and SPL conceived of and designed the experiments. TEC coordinated sorghum transformation, MG assembled the vector and ZG generated and confirmed the transgenic sorghum lines. WW performed sorghum copy number analysis. FA coordinated sugarcane transformation, BK and TN, generated and confirmed the transgenic sugarcane lines. NA and CES assembled the recombinant DNA vector for sugarcane, and performed experimental measurements. CES analyzed the data. CES and SPL wrote the manuscript with contributions and review from all authors.

Supporting Information

Fig. S1: Screening T1 transgenic sorghum lines.
Fig. S2: Screening T0 transgenic sugarcane lines.
Fig. S3: Gene expression in greenhouse and field grown sorghum.
Fig. S4: Normalized induction curves from greenhouse and field grown sorghum.
Fig. S5: Plant growth traits in greenhouse grown sorghum plants.
Fig. S6: Sorghum field experimental design and weather conditions.
Fig. S7: Steady-state BS leakiness of field grown sorghum.
Fig. S8: Normalized induction curves from greenhouse-grown sugarcane.
Fig. S9: Plant growth traits in greenhouse grown sugarcane plants.
Fig. S10: Average yield of sorghum and sugarcane over the last 20 to 30 years.
Fig. S11: Light intensity directly outside the greenhouse.
Table S1: List of primers used in this manuscript.
Table S2: Summary of harvest measurements and yield characterization of field-grown sorghum.
Table S3: Summary of leaf mass per area (LMA), chlorophyll content (SPAD value), leaf carbon and nitrogen content and total soluble protein (TSP) of sorghum and sugarcane plants.

730 **Table 1. Summary of biochemical and leaf gas exchange measurements from greenhouse grown**
731 **sorghum and sugarcane.** Values are shown as the mean ± SEM. Values significantly different from WT
732 at $P < 0.05$ are in bold. One-way ANOVA, Dunnett's post hoc test.

Parameter	WT	RBCS-RAF1 Hn1a	RBCS-RAF1 Zg12a	RBCS-RAF1 Zg5b	Sample number (*N*)
Sorghum - Greenhouse					
Initial Rubisco Activity ($\mu mol\ m^{-2}\ s^{-1}$)	13.48 ± 1.16	**19.00 ±1.45**	**22.28 ± 1.61**	17.60 ± 1.20	5-6
Rubisco Activation State (%)	71.41 ± 6.99	64.89 ± 4.47	79.21 ± 5.31	75.38 ± 5.79	5-6
ΦPSII	0.299 ± 0.002	**0.336 ± 0.007**	**0.331 ± 0.009**	**0.338 ± 0.006**	7-10
$V_{p,max}$ ($\mu mol\ m^{-2}\ s^{-1}$)	80.32 ± 7.38	88.33 ± 3.19	88.05 ± 3.59	89.99 ± 2.93	7-10
C_i ($\mu mol\ mol^{-1}$)	153.53 ± 2.36	142.53 ± 2.18	144.62 ± 3.55	144.50 ± 4.95	7-10
g_{sw} ($mol\ m^{-2}\ s^{-1}$)	0.411 ± 0.010	**0.463 ± 0.009**	**0.472 ± 0.012**	**0.472 ± 0.014**	7-10
$\bar{A}_{180}$ ($\mu mol\ m^{-2}\ s^{-1}$)	10.31 ± 1.17	**14.25 ± 1.10**	**13.99 ± 0.90**	12.83 ± 0.78	8-9
Parameter	WT	RBCS-RAF1 3	RBCS-RAF1 9	RBCS-RAF1 25	Sample number (*N*)
Sugarcane - Greenhouse					
Initial Rubisco Activity ($\mu mol\ m^{-2}\ s^{-1}$)	15.89 ± 0.86	**23.84 ± 2.84**	**23.74 ± 1.58**	20.35 ± 1.81	6
Rubisco Activation State (%)	82.30 ± 4.38	81.86 ± 4.54	87.22 ± 3.10	79.40 ± 7.51	6
ΦPSII	0.297 ± 0.012	0.319 ± 0.008	0.300 ± 0.009	0.326 ± 0.009	10
$V_{p,max}$ ($\mu mol\ m^{-2}\ s^{-1}$)	68.82 ± 4.55	85.70 ± 6.97	68.99 ± 3.02	79.93 ± 4.76	9-10
C_i ($\mu mol\ mol^{-1}$)	116.48 ± 8.61	113.76 ± 6.29	121.17 ± 4.47	118.55 ± 3.27	9-10
g_{sw} ($mol\ m^{-2}\ s^{-1}$)	0.252 ± 0.012	0.282 ± 0.006	0.282 ± 0.007	**0.305 ± 0.015**	9-10
$\bar{A}_{300}$ ($\mu mol\ m^{-2}\ s^{-1}$)	11.05 ± 2.26	17.78 ± 2.08	5.62 ± 1.95	15.38 ± 1.77	7-8
Time to 50% A_{MAX} (min)	3.36 ± 0.38	3.05 ± 0.27	**9.27 ± 1.62**	3.35 ± 0.26	6-8

733

734

References

1. FAO (2024) FAOSTAT. (Food and Agricultural Organization of the United Nations, Rome, Italy).
2. A. L. Healey *et al.*, The complex polyploid genome architecture of sugarcane. *Nature* 10.1038/s41586-024-07231-4 (2024).
3. F. G. Dohleman, S. P. Long, More Productive Than Maize in the Midwest: How Does Miscanthus Do It? *Plant Physiology* **150**, 2104-2115 (2009).
4. Y. He, D. Jaiswal, S. P. Long, X.-Z. Liang, M. L. Matthews, Biomass yield potential on U.S. marginal land and its contribution to reach net-zero emission. *GCB Bioenergy* **16**, e13128 (2024).
5. E. A. Heaton, F. G. Dohleman, S. P. Long, Meeting US biofuel goals with less land: the potential of Miscanthus. *Global Change Biology* **14**, 2000-2014 (2008).
6. S. Matsuoka, A. J. Kennedy, E. G. D. d. Santos, A. L. Tomazela, L. C. S. Rubio, Energy Cane: Its Concept, Development, Characteristics, and Prospects. *Advances in Botany* **2014**, 597275 (2014).
7. S. von Caemmerer, Updating the steady-state model of C4 photosynthesis. *Journal of Experimental Botany* **72**, 6003-6017 (2021).
8. B. J. Walker, A. VanLoocke, C. J. Bernacchi, D. R. Ort, The Costs of Photorespiration to Food Production Now and in the Future. *Annual Review of Plant Biology* **67**, 107-127 (2016).
9. M. Ermakova *et al.*, Installation of C4 photosynthetic pathway enzymes in rice using a single construct. *Plant Biotechnology Journal* **19**, 575-588 (2021).
10. R. Furbank, S. Kelly, S. von Caemmerer, Photosynthesis and food security: the evolving story of C4 rice. *Photosynthesis Research* **158**, 121-130 (2023).
11. M. E. Bianconi *et al.*, Continued adaptation of C4 photosynthesis after an initial burst of changes in the Andropogoneae grasses. *Systematic Biology* **69**, 445-461 (2019).
12. E. A. Ainsworth, S. P. Long, What have we learned from 15 years of free-air CO2 enrichment (FACE)? A meta-analytic review of the responses of photosynthesis, canopy. *New Phytologist* **165**, 351-371 (2005).
13. E. A. Ainsworth, S. P. Long, 30 years of free-air carbon dioxide enrichment (FACE): What have we learned about future crop productivity and its potential for adaptation? *Global Change Biology* **26**, 27-49 (2020).
14. A. D. B. Leakey, C. J. Bernacchi, F. G. Dohleman, D. R. Ort, S. P. Long, Will photosynthesis of maize (Zea mays) in the US Corn Belt increase in future CO2 rich atmospheres? An analysis of diurnal courses of CO2 uptake under free-air concentration enrichment (FACE). *Global Change Biology* **10**, 951-962 (2004).
15. A. D. B. Leakey *et al.*, Photosynthesis, productivity, and yield of maize are not affected by open-air elevation of CO2 concentration in the absence of drought. *Plant Physiology* **140**, 779-790 (2006).
16. A. P. de Souza, R. A. Arundale, F. G. Dohleman, S. P. Long, M. S. Buckeridge, Will the exceptional productivity of Miscanthus x giganteus increase further under rising atmospheric CO2? *Agricultural and Forest Meteorology* **171**, 82-92 (2013).
17. R. F. Sage, D. S. Kubien, Quo vadis C4? An ecophysiological perspective on global change and the future of C4 plants. *Photosynth Res* **77**, 209-225 (2003).
18. R. T. Furbank, Walking the C4 pathway: past, present, and future. *Journal of Experimental Botany* **67**, 4057-4066 (2016).
19. C. P. Pignon, S. P. Long, Retrospective analysis of biochemical limitations to photosynthesis in 49 species: C4 crops appear still adapted to pre-industrial atmospheric [CO2]. *Plant, Cell & Environment* **43**, 2606-2622 (2020).
20. S. von Caemmerer, R. T. Furbank, Strategies for improving C4 photosynthesis. *Current Opinion in Plant Biology* **31**, 125-134 (2016).

21. NOAA ((2024) Trends in Atmospheric Carbon Dioxide. (Global Monitoring Laboratory, NOAA, U.S. Department of Commerce, Boulder CO).
22. J. Ahn *et al.*, A record of atmospheric CO2 during the last 40,000 years from the Siple Dome, Antarctica ice core. *Journal of Geophysical Research: Atmospheres* **109**, D13305 (2004).
23. Y. Wang, K. X. Chan, S. P. Long, Towards a dynamic photosynthesis model to guide yield improvement in C4 crops. *The Plant Journal* **107**, 343-359 (2021).
24. Y. Wang *et al.*, Increased bundle-sheath leakiness of CO2 during photosynthetic induction shows a lack of coordination between the C4 and C3 cycles. *New Phytologist* **236**, 1661-1675 (2022).
25. R. T. Furbank *et al.*, Genetic Manipulation of Key Photosynthetic Enzymes in the C4 plant Flaveria bidentis. *Functional Plant Biology* **24**, 477-485 (1997).
26. C. E. Salesse-Smith *et al.*, Overexpression of Rubisco subunits with RAF1 increases Rubisco content in maize. *Nature Plants* **4**, 802-810 (2018).
27. C. E. Salesse-Smith, R. E. Sharwood, F. A. Busch, D. B. Stern, Increased Rubisco content in maize mitigates chilling stress and speeds recovery. *Plant Biotechnology Journal* **18**, 1409-1420 (2020).
28. D. K. Yoon *et al.*, Transgenic rice overproducing Rubisco exhibits increased yields with improved nitrogen-use efficiency in an experimental paddy field. *Nature Food* **1**, 134-139 (2020).
29. S. Von Caemmerer, *Biochemical models of leaf photosynthesis* (Csiro publishing, 2000).
30. S. P. Long *et al.*, Into the Shadows and Back into Sunlight: Photosynthesis in Fluctuating Light. *Annual Review of Plant Biology* **73**, 617-648 (2022).
31. R. A. Slattery, B. J. Walker, A. P. M. Weber, D. R. Ort, The Impacts of Fluctuating Light on Crop Performance. *Plant Physiology* **176**, 990-1003 (2018).
32. U. Feller, I. Anders, T. Mae, Rubiscolytics: fate of Rubisco after its enzymatic function in a cell is terminated. *Journal of Experimental Botany* **59**, 1615-1624 (2007).
33. A. I. Flamholz *et al.*, Revisiting Trade-offs between Rubisco Kinetic Parameters. *Biochemistry* **58**, 3365-3376 (2019).
34. R. F. Sage, A. D. McKown, Is C4 photosynthesis less phenotypically plastic than C3 photosynthesis? *Journal of Experimental Botany* **57**, 303-317 (2005).
35. C. P. Pignon, M. R. Lundgren, C. P. Osborne, S. P. Long, Bundle sheath chloroplast volume can house sufficient Rubisco to avoid limiting C4 photosynthesis during chilling. *Journal of Experimental Botany* **70**, 357-365 (2018).
36. G. Zhang *et al.*, The reference genome of Miscanthus floridulus illuminates the evolution of Saccharinae. *Nature Plants* **7**, 608-618 (2021).
37. R. F. Sage, Was low atmospheric CO_2 during the Pleistocene a limiting factor for the origin of agriculture? *Global Change Biology* **1**, 93-106 (1995).
38. K. Wostrikoff, D. Stern, Rubisco large-subunit translation is autoregulated in response to its assembly state in tobacco chloroplasts. *Proc Natl Acad Sci U S A* **104**, 6466-6471 (2007).
39. Y. Suzuki, A. Makino, Availability of Rubisco Small Subunit Up-Regulates the Transcript Levels of Large Subunit for Stoichiometric Assembly of Its Holoenzyme in Rice. *Plant Physiology* **160**, 533-540 (2012).
40. Y. Suzuki *et al.*, Increased Rubisco Content in Transgenic Rice Transformed with the 'Sense' rbcS Gene. *Plant and Cell Physiology* **48**, 626-637 (2007).
41. C. Hermida-Carrera, M. V. Kapralov, J. Galmés, Rubisco Catalytic Properties and Temperature Response in Crops. *Plant Physiology* **171**, 2549-2561 (2016).
42. C. Ishikawa, T. Hatanaka, S. Misoo, C. Miyake, H. Fukayama, Functional Incorporation of Sorghum Small Subunit Increases the Catalytic Turnover Rate of Rubisco in Transgenic Rice. *Plant Physiology* **156**, 1603-1611 (2011).

43. N. Salvatori, G. Alberti, O. Muller, A. Peressotti, Does Fluctuating Light Affect Crop Yield? A Focus on the Dynamic Photosynthesis of Two Soybean Varieties. *Frontiers in Plant Science* **13**, 862275 (2022).
44. J. Kromdijk *et al.*, Improving photosynthesis and crop productivity by accelerating recovery from photoprotection. *Science* **354**, 857-861 (2016).
45. S. H. Taylor *et al.*, Faster than expected Rubisco deactivation in shade reduces cowpea photosynthetic potential in variable light conditions. *Nature Plants* **8**, 118-124 (2022).
46. S. H. Taylor, S. P. Long, Slow induction of photosynthesis on shade to sun transitions in wheat may cost at least 21% of productivity. *Philos Trans R Soc Lond B Biol Sci* **372**, 1730 (2017).
47. S. Deschamps *et al.*, A chromosome-scale assembly of the sorghum genome using nanopore sequencing and optical mapping. *Nature Communications* **9**, 4844 (2018).
48. S. Belide, T. Vanhercke, J. R. Petrie, S. P. Singh, Robust genetic transformation of sorghum (Sorghum bicolor L.) using differentiating embryogenic callus induced from immature embryos. *Plant Methods* **13**, 109 (2017).
49. F. R. Miller, Registration of RTX430 sorghum parental line. *Crop Science* **24**, 1224-1224 (1984).
50. A. B. Cousins, Development of C4 photosynthesis in sorghum leaves grown under free-air CO2 enrichment (FACE). *Journal of Experimental Botany* **54**, 1969-1975 (2003).
51. A. B. Cousins *et al.*, Reduced photorespiration and increased energy-use efficiency in young CO₂-enriched sorghum leaves. *New Phytologist* **150**, 275-284 (2001).
52. G. W. Wall *et al.*, Elevated atmospheric CO₂ improved Sorghum plant water status by ameliorating the adverse effects of drought. *New Phytologist* **152**, 231-248 (2001).
53. M. J. Ottman *et al.*, Elevated CO₂ increases sorghum biomass under drought conditions. *New Phytologist* **150**, 261-273 (2001).
54. J. Sheen, Metabolic repression of transcription in higher plants. *The Plant Cell* **2**, 1027-1038 (1990).
55. X. M. Guo, Z. X. Ge, S. J. Sato, T. E. Clemente, "Sorghum: *Sorghum bicolor* " in Agrobacterium Protocols, Vol 1, 3rd Edition, K. Wang, Ed. (2015), vol. 1223, pp. 181-188.
56. K. Głowacka *et al.*, An evaluation of new and established methods to determine T-DNA copy number and homozygosity in transgenic plants. *Plant, Cell & Environment* **39**, 908-917 (2016).
57. S. Belide, T. Vanhercke, J. R. Petrie, S. P. Singh, Robust genetic transformation of sorghum (Sorghum bicolor L.) using differentiating embryogenic callus induced from immature embryos. *Plant Methods* **13** (2017).
58. Y. Taparia, M. Gallo, F. Altpeter, Comparison of direct and indirect embryogenesis protocols, biolistic gene transfer and selection parameters for efficient genetic transformation of sugarcane. *Plant Cell, Tissue and Organ Culture (PCTOC)* **111**, 131-141 (2012).
59. F. Altpeter, S. Sandhu, "Genetic Transformation – Biolistics" in Plant Cell Culture: Essential Methods, M. Davey, P. Anthony, Eds. (Wiley, Chichester, 2010), 10.1002/9780470686522.ch12, pp. 217-239.
60. M. G. Murray, W. F. Thompson, Rapid isolation of high molecular weight plant DNA. *Nucleic Acids Res* **8**, 4321-4325 (1980).
61. C. E. Salesse-Smith *et al.*, Greater mesophyll conductance and leaf photosynthesis in the field through modified cell wall porosity and thickness via <scp>AtCGR3</scp> expression in tobacco. *Plant Biotechnology Journal* 10.1111/pbi.14364 (2024).
62. S. M. Whitney, R. E. Sharwood, "Rubisco Engineering by Plastid Transformation and Protocols for Assessing Expression" in Chloroplast Biotechnology: Methods and Protocols, P. Maliga, Ed. (Springer US, New York, NY, 2021), 10.1007/978-1-0716-1472-3_10, pp. 195-214.

63. M. A. J. Parry *et al.*, Regulation of Rubisco by inhibitors in the light. *Plant, Cell & Environment* **20**, 528-534 (1997).
64. E. B. Lochocki ((2024) PhotoGEA: Photosynthetic Gas Exchange Analysis. v.0.11.0.
65. J. R. Evans, T. D. Sharkey, J. A. Berry, G. D. Farquhar, Carbon isotope discrimination measured concurrently with gas-exchange to investigate CO2 diffusion in leaves of higher-plants. *Australian Journal of Plant Physiology* **13**, 281-292 (1986).
66. S. von Caemmerer, O. Ghannoum, J. J. L. Pengelly, A. B. Cousins, Carbon isotope discrimination as a tool to explore C4 photosynthesis. *Journal of Experimental Botany* **65**, 3459-3470 (2014).